Indian Journal of Science and Technology, Vol 9(6), DOI: 10.17485/ijst/2016/v9i6/76607, February 2016
ISSN (Print) : 0974-6846
ISSN (Online) : 0974-5645

CHT Analysis of Trailing Edge Region Cooling In HP Stage Turbine Blade

Chandrakant R. Kini[1], Sai Sharan Yalamarty[1], Royston Marlon Mendonca[1], N. Yagnesh Sharma[1] and B. Satish Shenoy[2*]

[1]Department of Mechanical and Manufacturing Engineering, Manipal Institute of Technology, Manipal University, India; chandra.kini@manipal.edu, nysharma@hotmail.com, mendoncaroyston7@gmail.com, sai1494@yahoo.com

[2]Department of Aeronautical and Automobile Engineering, Manipal Institute of Technology, Manipal University, India; satish.shenoy@manipal.edu

Abstract

Gas turbines play a vital role in the today's industrialized society, and as the demands for power increase, the power output and thermal efficiency of gas turbines must also increase. Modern high-speed aero-engines operate at elevated temperatures about 2000 K to achieve better cycle efficiencies. The internal cooling techniques of the gas turbine blade includes: jet impingement, rib turbulated cooling, and pin-fin cooling which have been developed to maintain the metal temperature of turbine blades within acceptable limits. Cooling passages having fins are incorporated into the trailing edge regions which are modelled and analysed to achieve maximum thermal performance in terms of cooling. It is seen that fins provide an augmented convective area for better heat dissipation. The shape and orientation of fins plays a major role in air flow patterns and greatly affects the heat dissipation rate.

Keywords: CHT Analysis, Fins, HP Stage Turbine, Trailing Edge Cooling

1. Introduction

Gas turbines are highly effective engineered prime movers for converting energy from thermal form (combustion stage) to mechanical form, and are widely used for propulsion and power generation systems. One method of increasing both the power output and thermal efficiency is to increase the temperature of the gas entering the turbine section. In the advanced gas turbines of today, the turbine inlet temperature can be as high as 1500°C; however, this temperature exceeds the melting temperature of the metal blades.

From Brayton cycle it is known that the increase in pressure ratio and turbine inlet temperature increases the gas turbine thermal efficiency. However, increasing the pressure ratio beyond a certain value at any given firing temperature can actually result in lowering the overall cycle efficiency. As TIT increases, the heat transferred to the blades in the turbine also increases. The temperature level and variations on the turbine blade cause thermal stresses which must be limited to achieve reasonable durability goals.

2. Numerical Model

The commercial CFD software FLUENT (version6.3.26) from Fluent, Inc. is employed for analysis. The simulation uses the segregated solver, which employs an implicit pressure-correction scheme. The SIMPLE algorithm is used to couple pressure and velocity. Second order upwind scheme is selected for spatial discretization of the Reynolds Averaged Navier Stokes (RANS) equations as well as energy and turbulence equations. Converged results are obtained after the residuals were found to be less than the specified values. A converged result renders an energy residual of 10e-6, and momentum and turbulence kinetic energy residuals being 10e-5[1].

*Author for correspondence

2.1 Calculations

- Characteristic Length $L = \frac{2ab}{a+b} = \frac{2\times 0.026\times 0.012}{0.026+0.012}$
  $= 0.0164\text{m}$
- Velocity $V = \frac{\dot{m}}{\rho A} = \frac{\frac{90}{3600}}{0.54+0.000312} = 148.38\ \text{m/s}$
- Reynolds Number $R_{e=} \frac{\rho VL}{\mu} = \frac{0.54\times 148.38\times 0.0164}{3.186e-5}$
  $= 41246(>4000)$

Based on the above calculations, it is concluded that the flow is turbulent and hence k-ε model is chosen.

2.2 Equations of Flow

Continuity:

$$\frac{\partial}{\partial x_i}(\rho U_i) = 0 \tag{1}$$

Momentum:

$$\frac{\partial}{\partial x_j}(\rho U_i U_j) = \frac{\partial P}{\partial x_i} + \frac{\partial}{\partial x_j}\left[\mu\left(\frac{\partial U_i}{\partial x_j} + \frac{\partial U_i}{\partial x_i}\right) - \rho\overline{u_i u_j}\right] \tag{2}$$

Enthalpy:

$$\frac{\partial}{\partial x_j}(\rho U_i T) = \frac{\partial}{\partial x_j}\left[\frac{\frac{\mu}{\Pr}\partial T}{\partial x_j} - \rho\overline{u_i} t\right] \tag{3}$$

Energy:

$$\frac{\partial}{\partial x_j}\left[\rho u_j\left(h + \frac{1}{2}u_i^2\right)\right] - \frac{\partial}{\partial x_j}\left(k\frac{\partial T}{\partial x_j}\right) = 0 \tag{4}$$

Turbulence:

$$\frac{\partial}{\partial x_j}(\rho U_j k) = \frac{\partial}{\partial x_j}\left[\left(\mu + \frac{\mu_t}{\sigma_k}\right) - \frac{\partial k}{\partial x_j}\right] + P_k - \rho\varepsilon \tag{5}$$

Where,

$$P_k = -\rho\overline{u_i u_j}\left(\frac{\partial U_i}{\partial x_j}\right) \tag{6}$$

$$\frac{\partial}{\partial x_j}(\rho U_j \varepsilon) = \frac{\partial}{\partial x_j}\left[\left(\mu + \frac{\mu_t}{\sigma_\varepsilon}\right) - \frac{\partial \varepsilon}{\partial x_j}\right] + c_{\varepsilon 1}\frac{\varepsilon}{k}P_k - \rho c_{\varepsilon 2}\frac{\varepsilon^2}{k} \tag{7}$$

2.3 Boundary Conditions

A convective boundary condition of hot gas with free stream temperature of 1561 K[1,3] and convective heat transfer coefficient of 2028 W/m^{2}K[1,3]is applied to the blade surface. A mass flow rate of 90 kg/hr[1,3] is given at the inlet with a temperature of 644 K[1,3,5].

The material of the blade chosen is Nimonic Alloy 105[6] whose properties are shown in Table 1.

2.4 Grid Dependency

A line is chosen along the blade surface which is at 30 % chord length. Figure 1 shows grid dependence test based on mesh size to check the quality of mesh for solution accuracy. It is clear from the Figure 1 that temperature values do not deviate more than 1% between mesh sizes of 2.5 million cells and 1.4 million cells. Hence mesh size of 1.4 million cells is taken as the appropriate size due to reduced computational time.

3. Computational Domain for the Analysis

In the trailing edge, fins are introduced into the cooling passage to improve cooling. Three shapes are analysed to determine which would provide maximum and efficient cooling. A line is chosen along the blade surface which

Table 1. Thermal properties of blade

Properties	Units
Density	8010 kg/m^3
Specific heat	419 J/kg °C
Thermal Conductivity	10.89 W/m °C

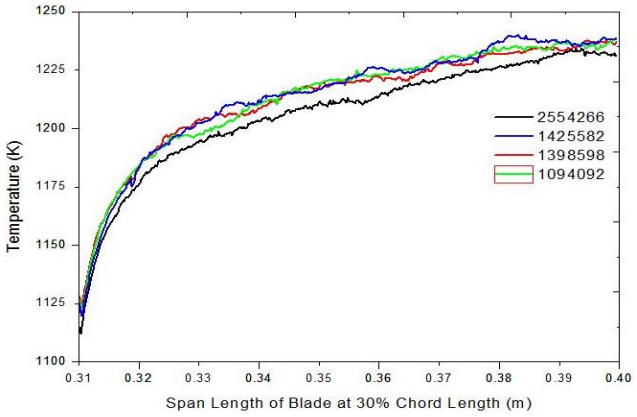

Figure 1. Grid dependency graph.

is at 70% chord length to compare each design based on temperature along the line.

3.1 Pin Fin

Three rows of pin fins are arranged in two patterns. The first includes fins arranged in an array, and in the second, fins are arranged in a staggered pattern as shown in Figure 2. Analysis is performed to determine the most effective pattern which would be followed for the other shapes. Based on the concept of increased surface area resulting in increased heat transfer, diameters of the fins are varied to determine the effect on thermal performance.

3.2 Triangular Fins

Triangular fins are modelled by maintaining the cross-sectional area constant. Additionally, the fins are arranged in four orientations to optimize air flow and provide the best thermal performance. Study of orientation of fins is important since air flow can be studied which helps to analyse flow pattern, obstructions in flow, and the variation of turbulence. The orientations are shown in Figure 3.

3.3 Airfoil Fins

Airfoils are well known for their aerodynamics. Similar to the triangular fins, the airfoil fins are arranged in the same four orientations. The orientations are shown in Figure 4. Fins are created in the trailing edge to increase heat transfer, thus improving cooling. Three shapes and four orientations are analysed. Different models are compared based on temperature and airflow around the fins and within the blade.

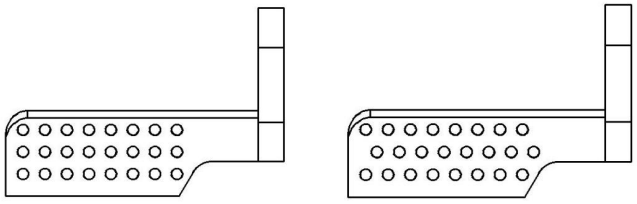

Figure 2. **(A)** Array arrangement of fins, **(B)** Staggered arrangement of fins.

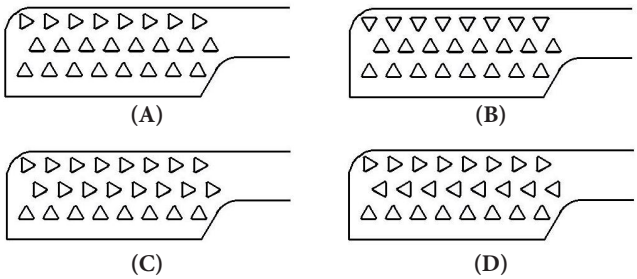

Figure 3. Triangular fins - **(A)** Orientation 1, **(B)** Orientation 2, **(C)** Orientation 3, **(D)** Orientation.

4. Results and Discussions

4.1 Pin Fin

From Table 2, it is seen that staggered arrangement of fins is better than that of array. This can be clearly justified by Figure 5 and Figure 6 which shows the temperature plot and cooling efficiency respectively, and Figure 7 which

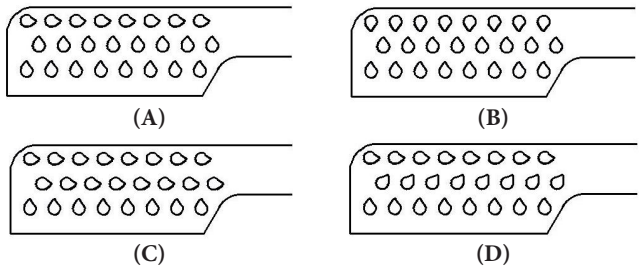

Figure 4. Airfoil fins - **(A)** Orientation 1, **(B)** Orientation 2, **(C)** Orientation 3, **(D)** Orientation 4.

Table 2. Comparison between array and staggered arrangement of fins

Sl. No.	Arrangement	Line Temperature (K)		Area weighted average (K)
		Min	Max	
1	Array	1044.082	1321.025	960.5286
2	Staggered	1029.864	1320.822	955.36

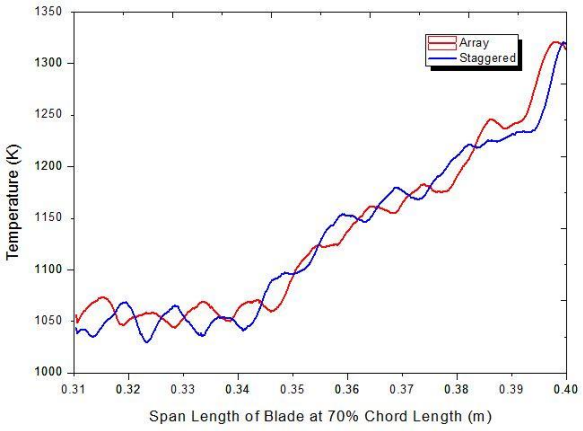

Figure 5. Temperature plot of array and staggered arrangement of fins.

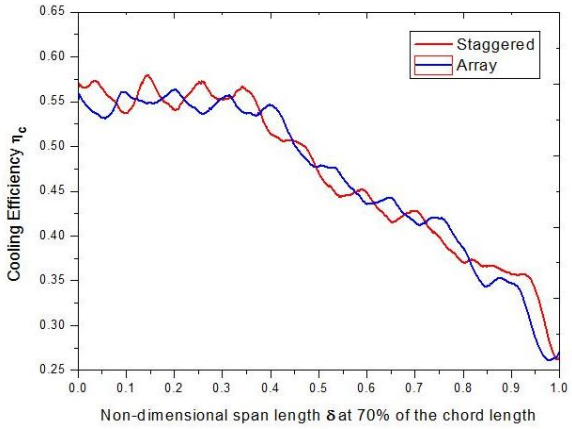

Figure 6. Cooling Efficiency along the span length of the blade for array and staggered arrangement of fins.

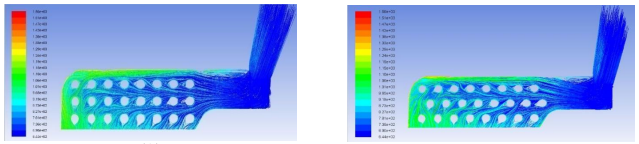

(A) **(B)**

Figure 7. Pathlines for arrangement of fins **(A)** Array, **(B)** Staggered.

shows the path lines of air in the cooling channel. In an array arrangement of fins, when the incoming air comes in the contact with the first few rows of fins, velocity reduces and is unable to cool the fins which are further ahead. This causes higher temperatures at the top of the blade resulting in majority of the blade being hotter. However, in a staggered arrangement, fins are placed in a triangular manner which causes air to come in contact with the first few rows and divert outward (towards the adjacent columns of fins). This results in a cooler blade surface.

4.1.1 Diameter Analysis

A diameter analysis is performed and from Table 3 and from Figure 8, it is found that 5mm provides the best thermal performance. While 7mm seems to be the best due to highest surface area, it resulted in the restriction of airflow due to narrow gaps between the fins, this can be seen in Figure 10. Hence, 5mm is better due to high surface area as well as smooth airflow around the fins, which can be concluded from Figure 9 (cooling efficiency graph).

4.2 Triangular Fins

From the Table 4 and Figure 11, it is seen that deciding the most effective orientation is very difficult if only line

Table 3. Diameter analysis of pin fins

Sl. No.	Diameter (mm)	Line Temperature (K)		Area weighted average (K)
		Min	Max	
1	1	1010.46	1406.07	960.38
2	3	1000.75	1347.46	955.36
3	5	1029.86	1320.82	955.28
4	7	1054.83	1327.9	970.1232

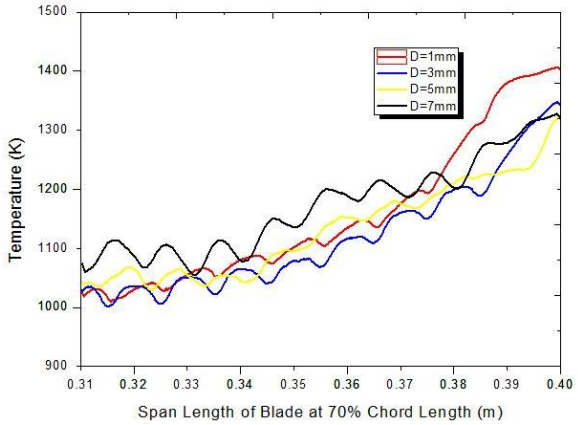

Figure 8. Temperature plot of varying diameters.

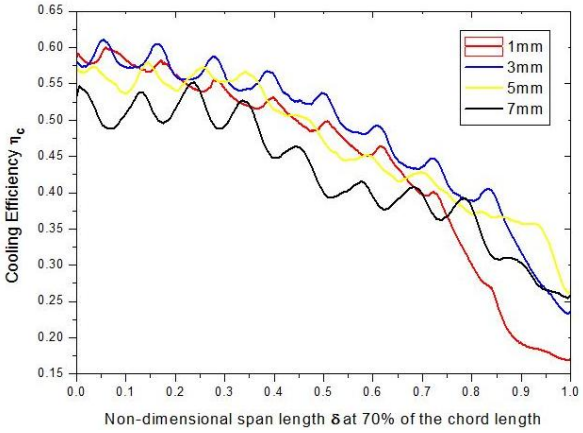

Figure 9. Cooling Efficiency along the span length of the blade for varying diameters of fins.

temperature is used as a parameter, hence, along with line temperature, area weighted average and airflow patterns play a crucial role in determining the optimum orientation. While the aim is to reduce the highest temperature on the blade, it's also important to cool the entire blade surface. Therefore, the parameters for each orientation are compared and from Figure 12, orientation 3 proves

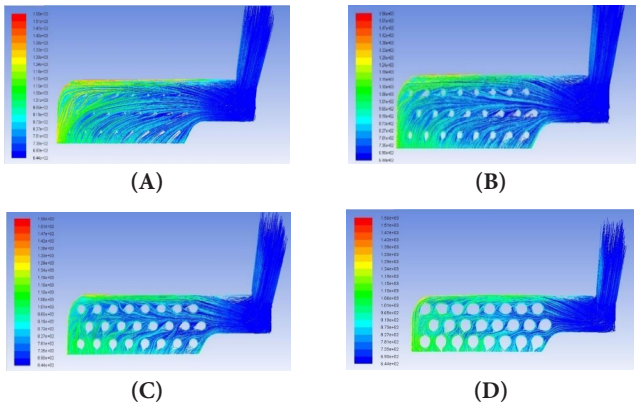

Figure 10. Pathlines for varying diameters of pin fins **(A)** 1mm, **(B)** 3mm, **(C)** 5mm, **(D)** 7mm.

Table 4. Comparison between Orientations of Triangular Fins

Sl. No.	Orientation	Line Temperature (K)		Area weighted average (K)
		Min	Max	
1	1	1071.33	1206.95	966.16
2	2	1064	1240.75	966.39
3	3	1068.08	1214.09	965.78
4	4	1046.04	1238.02	966

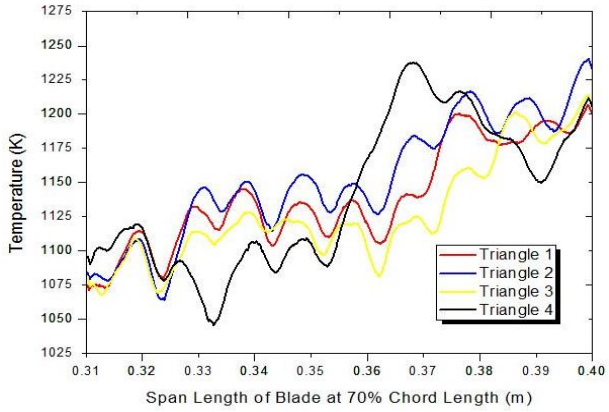

Figure 11. Temperature plot of different orientations of triangular fins.

to be the most effective orientation. Figure 13 shows the airflow patterns within the cooling channels.

4.3 Airfoil Fins

Similar to triangular fins, it's difficult to decide the optimum orientation from line temperatures in Table 5. Hence, line temperatures, area weighted average and cooling efficiency considered together, give a clearer idea about the

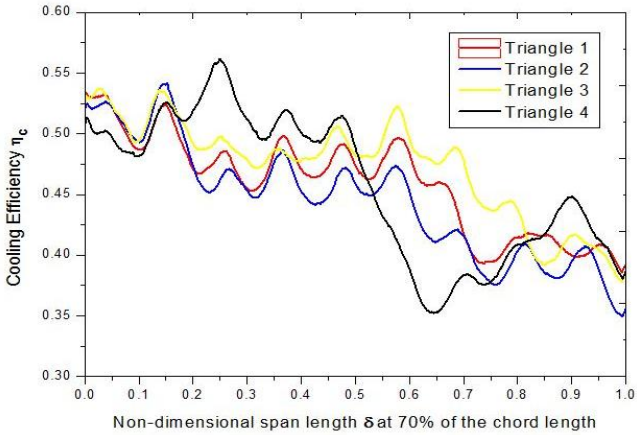

Figure 12. Cooling Efficiency along the span length of the blade for different orientations of triangular fins.

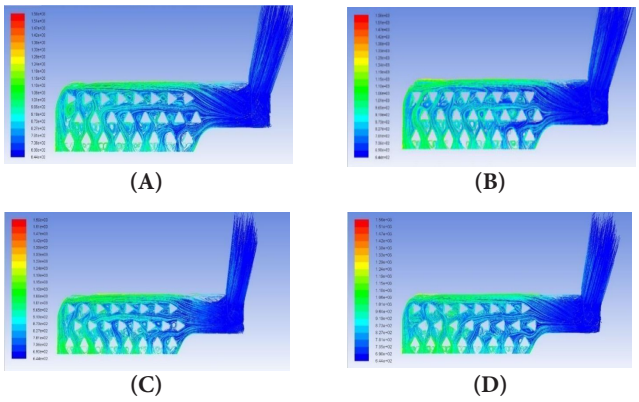

Figure 13. Pathlines for triangular fins – **(A)** Orientation 1 **(B)** Orientation 2 **(C)** Orientation 3 **(D)** Orientation 4.

Table 5. Comparison between Four Orientations of Airfoil Fins

Sl. No.	Orientation	Line Temperature (K)		Area weighted average (K)
		Min	Max	
1	1	1060.39	1300	958.79
2	2	1051.56	1245.75	960.3
3	3	1040.36	1262.7	957.03
4	4	1045.05	1255.78	955.4

optimum orientation. Figure 16 shows the airflow around the fins as well as temperature distribution. While orientation 3 was the best for triangular fins, it's not necessary that the same orientation would have the same effect on different shapes. This is because every shape diverts and directs flow in different patterns, thus making it important

to analyse all orientations for every shape. For airfoil fins, from Figure 14 and Figure 15. It can be seen that orientation 4 provides the least temperatures across the blade, hence orientation 4 is chosen as the optimum one.

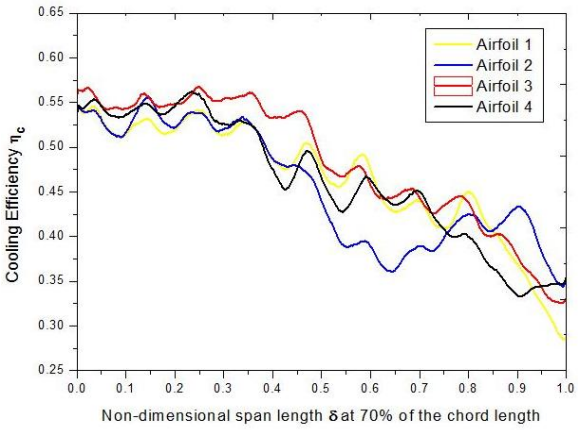

Figure 14. Cooling Efficiency along the span length of the blade for different orientations of airfoil fins.

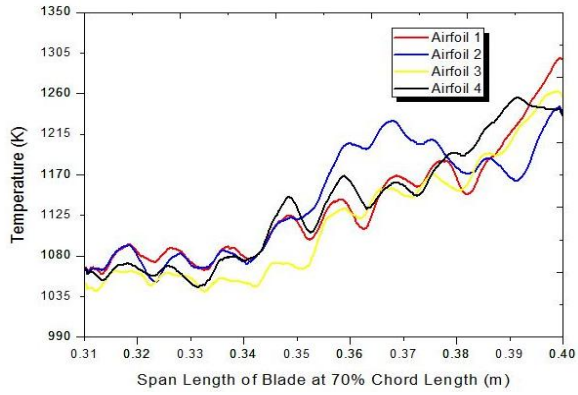

Figure 15. Temperature plot of different orientations of airfoil fins.

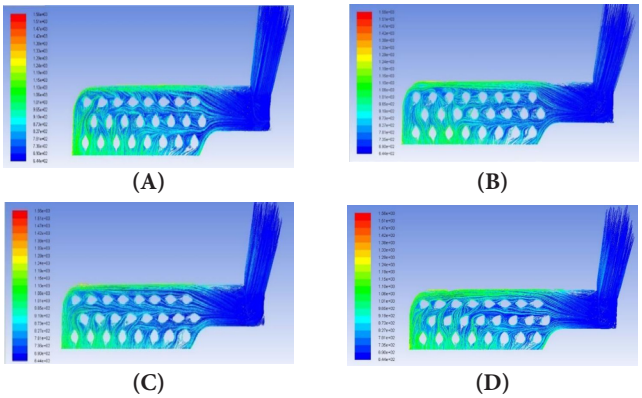

Figure 16. Pathlines for airfoil fins – **(A)** Orientation 1 **(B)** Orientation 2 **(C)** Orientation 3 **(D)** Orientation 4.

5. Conclusions

From the present study the following conclusions are drawn.

- It is seen that fins provide an augmented convective area for better heat dissipation.
- The fins also act as hindrances which disrupts the smooth flow of air, hence increasing turbulence. This increased turbulence improves heat dissipation rate.
- The shape and orientation of fins plays a major role in air flow patterns. This can greatly affect the heat dissipation rate.
- The temperature plots have a wavy nature because of the presence of equally spaced fins within the blade.

6. Nomenclature

TIT – Turbine inlet temperature in K
$\dot{m}$ – Mass flow rate of coolant air in kg/hr
ρ – Density of coolant air in kg/m^3
A – Area of inlet duct in mm^2
μ – Dynamic Viscosity of coolant air
R_e – Reynolds Number

7. References

1. Kini CR, Shenoy SB, Sharma YN. Thermo-structural analysis of HP stage gas turbine blades having helicoidal cooling ducts. International Journal of Advancements in Mechanical and Aeronautical Engineering. 2014; 1(2):57–60.
2. Kini CR, Shenoy SB, Sharma YN. Numerical Analysis of Gas Turbine HP Stage Blade Cooling with New Cooling Duct Geometries. International Journal of Earth Sciences and Engineering. 2012; 05(02):1057–62.
3. Kini CR, Shenoy SB, Sharma YN. Computational Conjugate Heat Transfer Analysis of HP Stage Turbine Blade Cooling: Effect of Turbulator Geometry in Helicoidal Cooling Duct. World Academy of Science Engineering and Technology Special Journal Issue. 2012; 70:645–52.
4. Kini CR, Shenoy SB, and Sharma YN. A Computational Conjugate Thermal Analysis of HP Stage Turbine Blade Cooling with Innovative Cooling Passage Geometries. Journal of Lecture Notes in Engineering and Computer Science. 2011; 1(2192):2168–73.
5. Adrian T. Plesca, Power Losses and Thermal Analysis of Power Rectifiers. Indian Journal of Science and Technology. 2013; 6(7):4976–82.
6. Material Properties [Online]. Available from: www.specialmetals.com/documents/Nimonic% 20alloy%20105.pdf, 11/08/2010